Nano Energy 82 (2021) 105695

Contents lists available at ScienceDirect

Nano Energy

journal homepage: http://www.elsevier.com/locate/nanoen

Single electrode piezoelectric nanogenerator for intelligent passive daytime radiative cooling

Wei-Zhi Song [a], Xiao-Xiong Wang [a], Hui-Jing Qiu [a], Ning Wang [a], Miao Yu [a,c], Zhiyong Fan [b], Seeram Ramakrishna [d], Han Hu [e], Yun-Ze Long [a,f,*]

[a] Collaborative Innovation Center for Nanomaterials & Devices, College of Physics, Qingdao University, Qingdao 266071, China
[b] Department of Electronic & Computer Engineering, The Hong Kong University of Science & Technology, Kowloon, Hong Kong, China
[c] Department of Mechanical Engineering, Columbia University, New York, NY 10027, USA
[d] Center for Nanofibers & Nanotechnology, National University of Singapore, Singapore
[e] State Key Laboratory of Heavy Oil Processing, College of Chemical Engineering, China University of Petroleum (East China), Qingdao 266580, China
[f] Collaborative Innovation Center for Eco-Textiles of Shandong Province, and State Key Laboratory of Bio-Fibers and Eco-Textiles, Qingdao University, Qingdao 266071, China

ARTICLE INFO

Keywords:
Passive daytime radiative cooling
Electrospinning
Piezoelectric nanogenerator
Energy harvesting
Self-monitoring

ABSTRACT

Passive daytime radiative cooling (PDRC) can cool down objects by simultaneously reflecting sunlight and radiating heat to the cold external space, which has no energy consumption. Traditional PDRC design usually needs to rely on micro-nano structures, which are easily damaged and lose function. On the one hand, the mechanical strength of PDRC can be enhanced. On the other hand, by integrating self-monitoring character in the same membrane fault part can be easily distinguished for fixing or replacing. Monitoring the damage by using traditional sensors will cause additional energy loss. Therefore, an intelligent PDRC that can monitor the failure itself is urgently needed to be developed. Here we found that the polyvinylidene fluoride-co-hexafluoropropylene (PVDF-HFP) nanofiber membrane obtained by electrospinning technology can effectively scatter sunlight, while emitting infrared rays matching the atmospheric window to achieve effective heat dissipation. In the preparation process, the electrostatic field can effectively polarize the PVDF-HFP to obtain good piezoelectric performance, which can be used to monitoring the integrity of membrane function. Meanwhile, the membrane can be used as a nanogenerator to collect mechanical energy in the environment, such as raindrop energy when used on the roof, thereby not only reducing cooling energy loss, but also collecting energy additionally, achieving a dual energy-saving design. Its excellent self-cleaning and recyclable characteristic bring more benefits to its green and energy-saving features. Therefore, this intelligent PDRC provides ideas for new energy-saving designs. At the same time, a simple preparation method is more conducive to the promotion of this technology.

1. Introduction

Passive daytime radiative cooling (PDRC) is an emerging effective cooling method [1–4]. The principle of this method is to scatter/reflect sunlight as much as possible to avoid temperature rise caused by sunlight absorption. On the other hand, the material needs to have good infrared emission in the atmospheric window band so that heat can be radiated to the cold outer space through the atmospheric window to achieve spontaneous cooling. Spontaneous cooling without power input makes this method very attractive. The micro-nano structure can provide a large number of material-air interfaces. On the one hand, the interfaces can effectively scatter sunlight, on the other hand, it provides more infrared emission interfaces. Therefore, in recent years, various macro and micro structures have been designed to achieve passive daytime radiative cooling. Micro-nano processings such as electron beam lithography RF-sputtering [5] were used to prepare metamaterials [6–8], photonic crystals [9–11], multilayer photonic structures [12–14], dielectrics, polymers and polymer dielectric composites [15,16] on metal mirrors. Although these designs are effective, expensive manufacturing costs and complex manufacturing techniques greatly limit their mass production and application. On the other hand, materials with micro-nano structures are generally vulnerable. In particular, it is applied to outdoor open air environment, which is extremely easy to cause local failure and affect heat dissipation under the influence of

* Corresponding author at: Collaborative Innovation Center for Nanomaterials & Devices, College of Physics, Qingdao University, Qingdao 266071, China.
E-mail addresses: yunze.long@qdu.edu.cn, yunze.long@163.com (Y.-Z. Long).

https://doi.org/10.1016/j.nanoen.2020.105695
Received 7 September 2020; Received in revised form 17 November 2020; Accepted 10 December 2020
Available online 13 January 2021

natural factors and human factors. This calls for an intelligent PDRC with simple production process, low cost, and the ability to monitor its own faults, which can accurately locate the damaged area for easy maintenance.

Recent PDRC designs use SiO_2 to be transparent to visible light, so visible light that is not reflected at the interface will not cause a sharp temperature rise, so nano-structured SiO_2 spheres can perform second and third refraction/reflection to effectively scatter visible light; and at the same time SiO_2 can also effectively emit infrared light, so it is widely used in combination with other materials to achieve effective PDRC design [15,17]. In addition, some organic materials such as polyvinylidene fluoride-co-hexafluoropropylene (PVDF-HFP) microporous structure are also used for PDRC design [1]. Based on the above principles, it is conceivable that the fiber membrane with disordered structure prepared by electrospinning technology is full of fiber-air interfaces, which scatters visible light and emits infrared light efficiently [17]. More importantly, we have designed an electrospinning single-electrode piezoelectric structure [18] to effectively monitor the performance of the membrane using advantages of piezoelectric materials [19,20]. At the same time, single-electrode configuration also avoids the influence of the top electrode shielding of the traditional two-electrode sensor on the PDRC heat dissipation effect, which has a huge influence on the optical properties of the upper surface. Electrospinning is a mature technology that has been widely used [21–25]. It relies on electrostatic repulsion between surface charges to prepare fiber materials [26,27] Compared with other nanostructure assemble methods, electrospinning has low cost, simple operation, high efficiency, mass production, and controllable structural parameters such as the shape and size of the prepared material [28,29]. The high-voltage electrostatic field in the spinning process can pre-polarize the fiber, which significantly improves the piezoelectric performance of the fiber [30,31]. After being assembled into a nanogenerator, the mechanical energy in the environment can be well collected to achieve a dual energy-saving design [32]. At the same time, self-powered sensing [18] is realized to achieve the purpose of monitoring its own faults.

Here, we demonstrate an intelligent PDRC dual energy-saving design based on electrospinning PVDF-HFP fiber that can monitor its own faults. The single-electrode piezoelectric configuration realizes the monitoring of its own working state. By dropping the top electrode, the smooth fiber surface can efficiently reflect sunlight. Its infrared emission peak can also transfer heat to space through the atmospheric window. Its passive daytime radiative cooling capacity has been experimentally proven. On the other hand, its good piezoelectric performance has also been confirmed, which can realize self-powered pressure monitoring and complete the monitoring of PDRC integrity. At the same time, it also successfully collected the mechanical energy of raindrops and realized the double energy-saving design. In addition, its good self-cleaning ability, recyclability, simple preparation method and mechanical properties are also conducive to its practical application.

2. Experiment and characterization

2.1. Materials

PVDF-HFP pellets (Mw~450,000, Sigma-Aldrich LLC.) was used in this work. N, N-Dimethylformamide (DMF) was obtained from Sinopharm Chemical Reagents. Acetone was obtained from the Laiyang Fine Chemical Factory, China.

2.2. Preparation of solutions and electrospinning

A PVDF-HFP solution was prepared by dissolving PVDF-HFP pellets (20 wt%) in an acetone–DMF solvent mixture (1/1 w/w) and then stirring the mixture with a magnetic stir bar for 4 h at 45 °C. Finally, a hand-held electrospinning device [33] is used to electrospin, as shown in Fig. 1a. The spinning distance is controlled at 10–20 cm. The purpose of this manufacturing process is to quickly produce coating materials with high yields and high uniformity.

Fig. 1b shows the molecular structure of PVDF-HFP before and after electrospinning. During the electrospinning process, part of the PVDF in the PVDF-HFP is changed from the α phase to the β phase, so that the PVDF-HFP fiber has piezoelectric characteristics [34]. Fig. 1c is a photograph of a PVDF-HFP membrane and representative SEM images. The nanofiber diameter distribution is shown in Fig. 1d. The fiber diameter is normally distributed in the range of 0.2–1.8 μm, which is the same as the wavelength of visible light and near-infrared light.

2.3. Characterizations

SEM (TM-1000) was used to characterize the morphology and

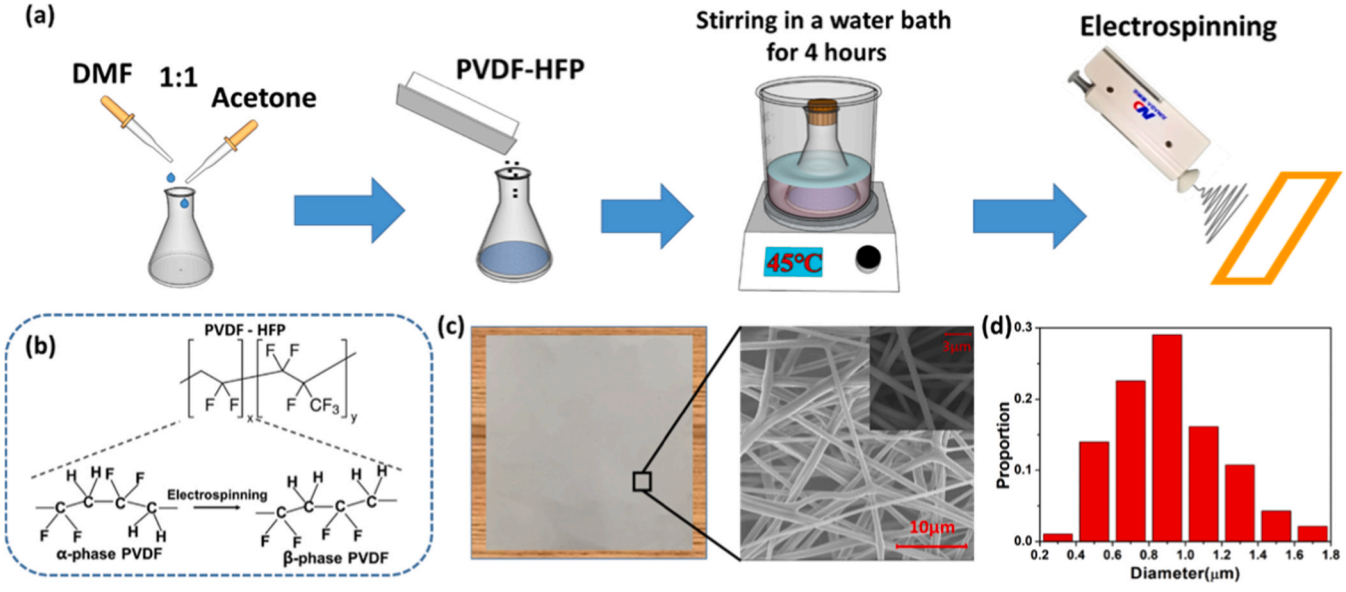

Fig. 1. The formation and morphology characterization of the dual energy-saving PVDF-HFP fiber membrane. (a) The preparation process of the PVDF-HFP fiber membrane. (b) Changes in PVDF-HFP molecular structure during electrospinning. (c) The photograph of PVDF-HFP membrane and representative SEM images. (d) The diameter distribution of PVDF-HFP fiber in the membrane.

dimensions of the PVDF-HFP fibers. The digital multimeter (Rigol DM 3058) nanovoltmeter (Keithley 2182) and temperature probe (UT-T12) were used to monitor the temperature change of the experimental group and the control group in real time. Ultraviolet visible near infrared spectrophotometer and Fourier transform infrared spectrometer (Nicolet iS10) was used to test the spectrum of the membrane in different bands. COMSOL was used to simulate the reflectivity of PDRC to sunlight at different angles and the effect of heat dissipation. The digital multimeter was also used to measure changes in capacitor voltage. Low noise current amplifier (SR570) and digital oscilloscope (GDS-2102) were used to record piezoelectric current and voltage. The mechanical properties of PVDF-HFP membrane was measure by Instron 3300 Universal Testing Systems. JY-PHb optical contact angle meter was used to test the water contact angle of membrane.

3. Results and discussion

3.1. Passive daytime radiative cooling

At temperature T, the net cooling power P_{cool} of the radiant cooler with area A is given by [14].

$$P_{cool}(T) = P_{rad}(T) - P_{atm}(T_{amb}) - P_{Sun} - P_{cond+conv} \quad (1)$$

$$P_{rad}(T) = \mathrm{A}\int d\Omega\cos\theta \int_0^\infty d\lambda I_{BB}(T,\lambda)\epsilon(\lambda,\theta) \quad (2)$$

$$P_{atm}(T_{amb}) = \mathrm{A}\int d\Omega\cos\theta \int_0^\infty d\lambda I_{BB}(T,\lambda)\epsilon(\lambda,\theta)\epsilon_{atm}(\lambda,\theta) \quad (3)$$

$$P_{Sun} = \mathrm{A}\int_0^\infty d\lambda\epsilon(\lambda,\theta_{Sun})I_{AM1.5}(\lambda) \quad (4)$$

$$P_{cond+conv}(T,T_{amb}) = Ah_c(T_{amb}-T) \quad (5)$$

where $P_{rad}(T)$ is the power radiated out by the structure, $I_{BB}(T,\lambda)$ is the spectral radiance of a blackbody at temperature T, $\epsilon(\lambda,\theta)$ is the spectral and angular emissivity, $P_{atm}(T_{amb})$ is the absorbed power from the atmosphere radiation, P_{Sun} is the incident solar power absorbed, $I_{AM1.5}(\lambda)$ is the solar illumination, $P_{cond+conv}$ is the power lost due to convection and conduction, $h_c = h_{cond} + h_{conv}$ is a combined non-radiative heat coefficient.

In order to achieve daytime radiative cooling, the equipment must meet the power balance equation of Eq. (1). First, in order to minimizeP_{Sun}, it must reflect sunlight strongly. Since the solar spectrum is mainly distributed in 0.3–2.5 μm, it must reflect strongly in the visible and near-infrared wavelength range. Secondly, it must emit heat radiation strongly to increase $P_{rad}(T)$ as much as possible，while minimizing incident atmospheric thermal radiation $P_{atm}(T_{amb})$ by minimizing its emission at non-atmospheric window. Therefore, the device must only selectively and strongly emit light at atmospheric windows between 8 and 13 μm and 19–22 μm, and reflect at all other wavelengths [14].

Fig. 2a is the principle of passive daytime radiative cooling. The

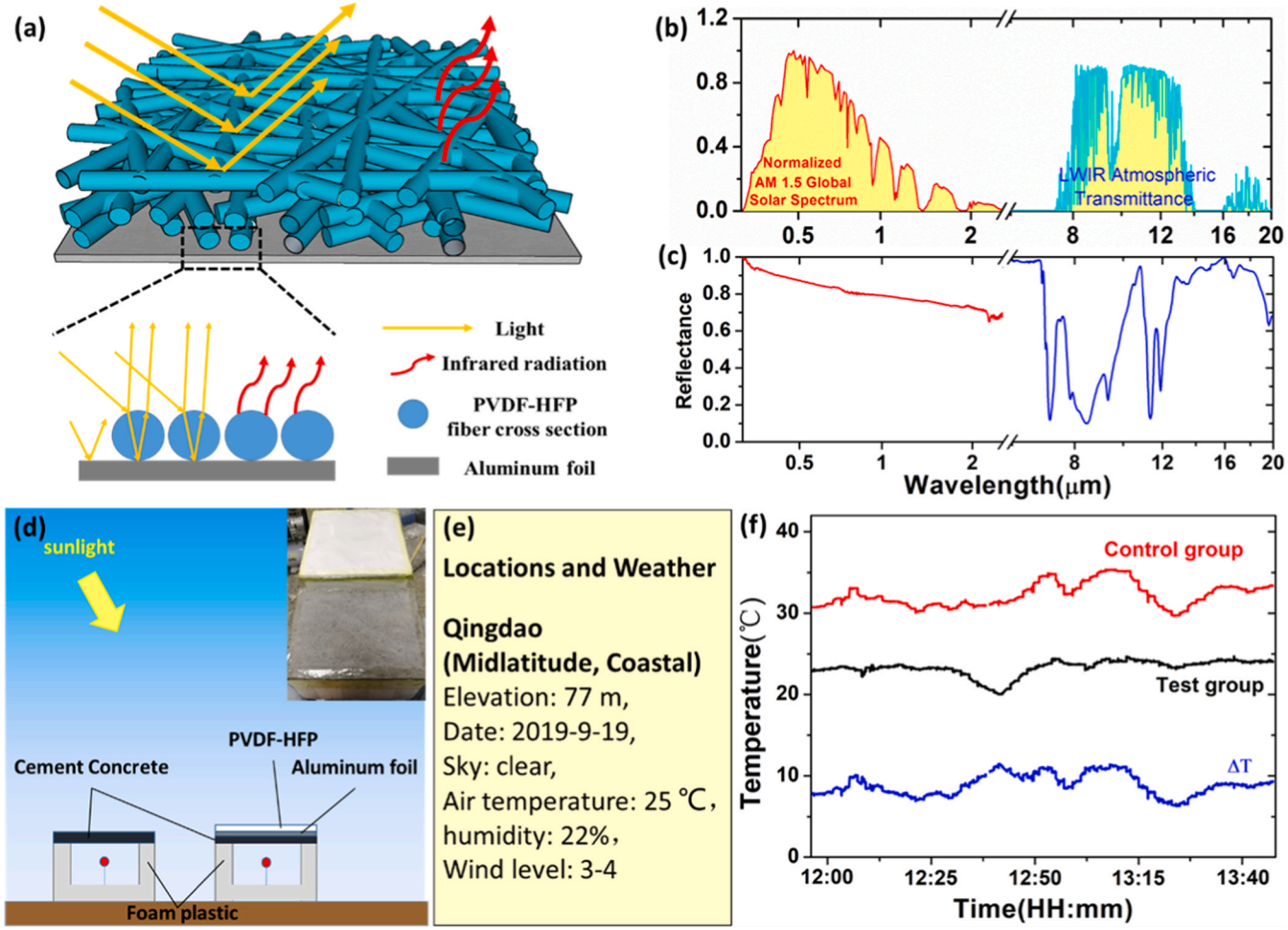

Fig. 2. The optical properties and passive daytime radiative cooling performance of PVDF-HFP membrane. (a) The schematic of cooling principle. (b) Normalized AM 1.5 global solar spectrum and long-wave infrared atmospheric transmittance. (c) Spectral reflectance of PVDF-HFP membrane. (d) Schematic diagram of a device for testing performance in sunlight. (e) Topographic and meteorological information of the test locations. (f) Temperature data of the result for Qingdao.

different vibration modes of the material's molecular structure make the material have strong thermal emissivity. Micro and nano fibers in the membrane can effectively scatter sunlight, thereby reducing indoor temperature. Fig. 2b shows the normalized AM 1.5 global solar spectrum and long-wave infrared atmospheric transmittance. The absorbance of the atmosphere causes a sharply varying in the spectrum. However, the first atmospheric transmission window of 8–13 μm and the second atmospheric window of 16–20 μm make passive radiative cooling possible. It can be seen from Fig. 2c, spectral reflectance of PVDF-HFP membrane, that the high solar reflectance in the visible and near-infrared region of 0.3–2.5 μm can ensure that all incident light is well reflected. The emissivity/absorptivity of 7–13 μm and 16–20 μm can correspond to the atmospheric window to achieve passive radiative cooling.

In order to test the actual effect of heat dissipation, a controlled experiment was designed, as shown in Fig. 2d. Two equal-volume plastic foam boxes were used to reduce heat transfer, and a cement concrete roof was used to simulate a real roof. The top layer of the experimental group was covered with aluminum foil and PVDF-HFP fiber membrane. PVDF-HFP fiber plays the role of reflecting sunlight and emitting infrared rays. Residual transmitted light can be reflected by aluminum foil. At the same time, aluminum foil can also work as the electrode material of single-electrode nanogenerator. During PDRC test, the location and weather information of the test is listed in Fig. 2e. The results in Fig. 2f show that the PVDF-HFP fiber membrane dropped temperature in the box lower by about 10 °C than the control group, achieving a sub-ambient temperature drop. The comparison with the ambient temperature is shown in Fig. S6. This simulation shows that PVDF-HFP fiber membrane can reduce the temperature in the building, thereby reducing the cost of air conditioning. And its performance in passive daytime radiative cooling is comparable to the results in other literatures. As shown in Table S1.

To verify the reliability of the experimental data, a series of theoretical simulations were constructed through COMSOL. First, it can be inferred from the white appearance of the fiber membrane that it has a strong optical reflection of sunlight. COMSOL's simulation results also confirmed this (Fig. 3a). Randomly distributed cylindrical fibers cause diffuse reflection independent of the angle of incidence. In order to

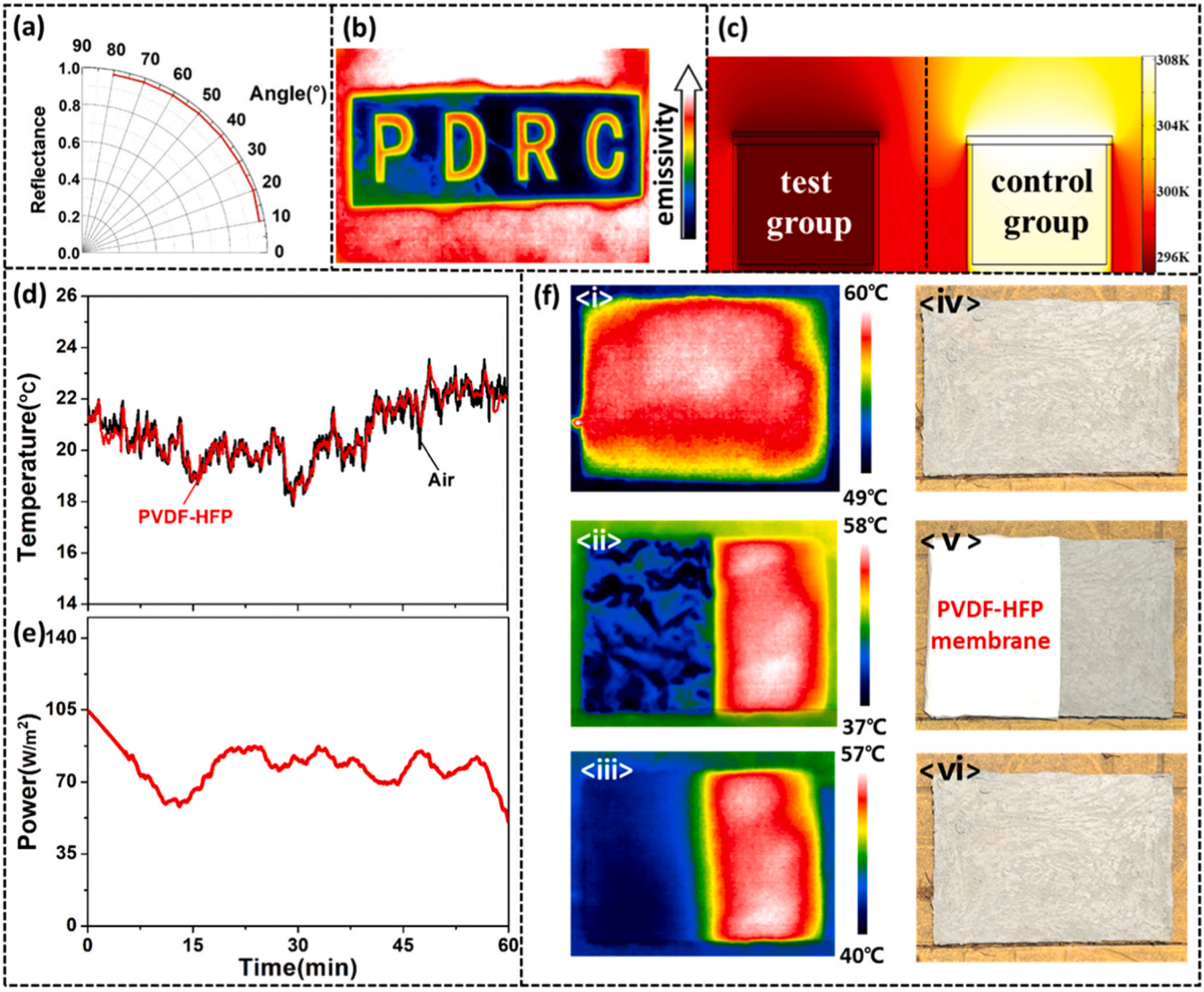

Fig. 3. (a) The reflectivity of PVDF-HFP fiber membrane to sunlight incident at different angles was simulated by COMSOL. (b) Infrared image of the radiant membrane, with a caved aluminum foil on the membrane as a reference (dark area). (c) Comparison of the heat dissipation capacity of the experimental group and the control group simulated by COMSOL. (d) Temperature tracking and (e) corresponding cooling power data. Additional information is provided in the Supplementary Materials S1. (f) Infrared images and corresponding digital images of concrete slabs in different states: <i, iv> placed in sunlight for 1 h to achieve thermal stability; <ii, v> cover coating; <iii, vi> the layer was removed after 1 h.

qualitatively check the mid-infrared emissivity of the fiber membrane, we took an infrared image of the PVDF-HFP fiber membrane with aluminum foil (low emissivity) placed on its surface as a reference. The wavelength range of the camera lens is 7.2–13 μm (mostly overlapping with the atmospheric window). The results show that the emissivity of the fiber membrane in this range is very high, as shown in Fig. 3b. The heat dissipation effect of the test group and the control group was simulated through the heat transfer module of COMSOL, as shown in Fig. 3c. In ordinary buildings without any protection, in the case of direct sunlight, a large amount of solar radiation can be absorbed by the roof, making the indoor temperature even higher than outdoor. The roof covered with PVDF-HFP fiber membrane can reflect most of the solar radiation energy, and radiate heat outward through the atmospheric window to reduce the indoor temperature.

Then, a temperature tracking method was used to characterize the heat dissipation power of the PDRC. When the peak solar intensity of Qingdao (China) on October 8 was 284 W m^{-2} and the weather was clear with low humidity (25%) and breeze (wind level 3), PVDF-HFP fiber membrane obtained a cooling powers of 78 W m^{-2}. The working principle is shown in Fig. S1. The temperature of the membrane is kept consistent with the air temperature by controlling the heating plate. The temperature curve as shown in Fig. 3d. Therefore, there is no heat conduction and heat convection. The heating power of the heater is the heat dissipation power of the PDRC (Fig. 3e). The infrared image shown in Fig. 3f further confirms the excellent cooling performance of the PVDF-HFP fiber membrane. After placing the concrete slab in direct sunlight to reach a thermally stable state (Fig. 3f <i, iv>), its left half was covered with PVDF-HFP fiber membrane (Fig. 3f <v>). After one hour, it reached thermal stability again (Fig. 3f <ii>), peeling off the fiber membrane and quickly taking an infrared photo (Fig. 3f <iii, vi>). As shown in Fig. 3f <iii>, the temperature of the left area of the concrete slab was significantly lower than that of the right area that did not covered anything, which fully proved its feasibility in practical application.

3.2. Integrating PDRC's self-monitoring capabilities

Traditional electronic devices often require two electrodes in order to be consistent with the acquisition circuit to maintain electrical neutrality. However, for PDRC materials, designing a two-electrode configuration will inevitably affect PDRC performance. The use of electrode pair perpendicular to the membrane surface will lead to a decrease in capacitance, resulting in a decrease in sensing accuracy. At the same time, this electrode configuration is also extremely difficult to

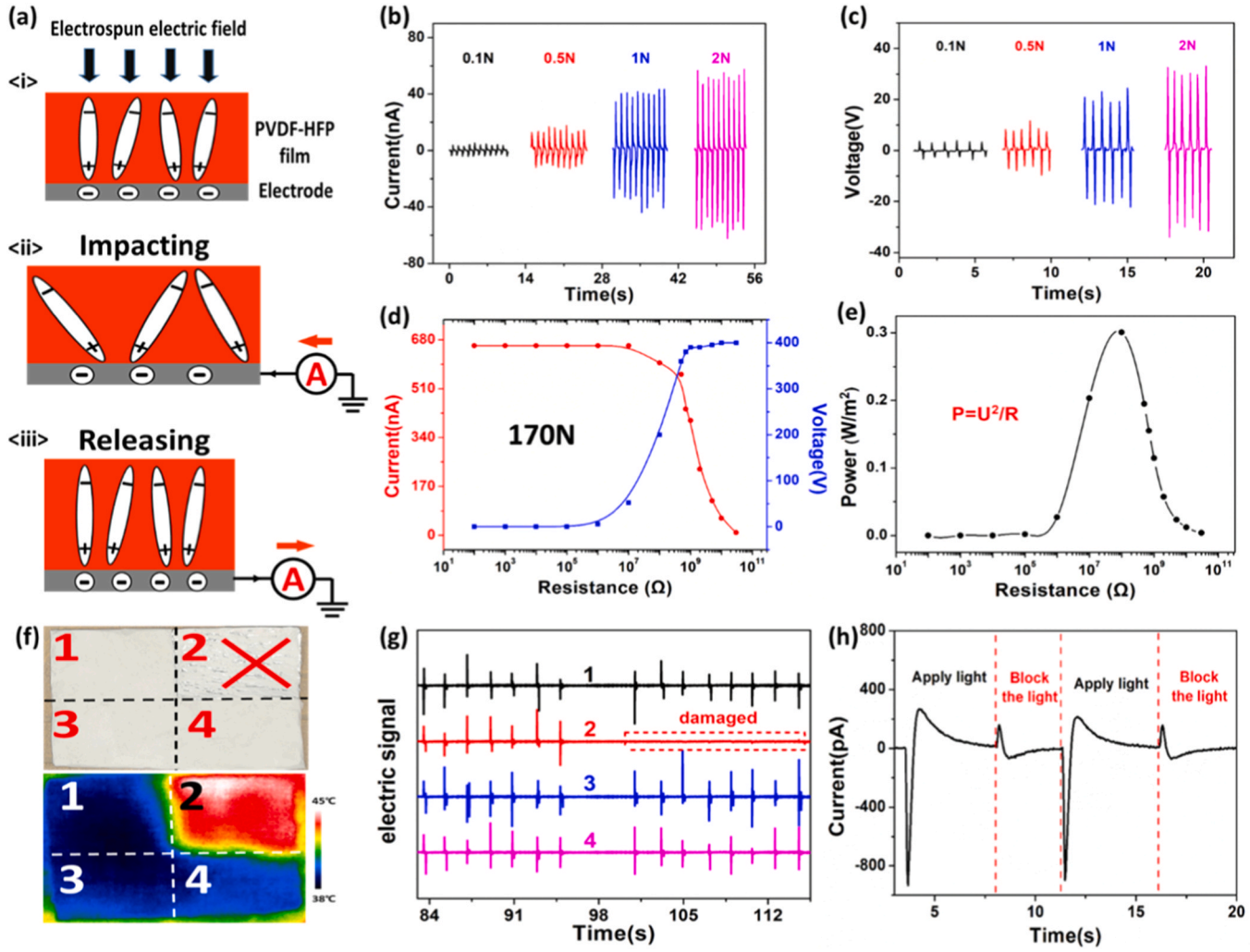

Fig. 4. Working mechanism and output performance of single-electrode intelligent PDRC. (a) The working mechanism of single-electrode intelligent PDRC. (b, c) Output current and voltage under different pressures. (d) Output current and voltage with various external load resistances. (e) Dependence of output power on load resistances. (f) Simulating a 2 × 2 PDRC array after the 2 area is destroyed, the heat dissipation effect of the corresponding area is also reduced. (g) The self-monitoring function is realized by comparing the electrical signal output of the four areas before and after damage. (h) The output signal changes before and after the radiator is blocked.

be constructed. When using top and bottom electrodes, the traditional metal electrode has a very low thermal emissivity and will not produce effective infrared emission, and will hinder the infrared of the PDRC layer emission. The transparency of transparent ITO is only for visible light, and its transmittance for infrared is not good. In fact, because piezoelectric materials work with displacement current, it is possible to design a single-electrode configuration, and this configuration has been confirmed in the previous work [18]. The working mechanism of a single-electrode piezoelectric nanogenerator is shown in Fig. 4a. During the electrospinning process, some PVDF-HFPs will spontaneously polarize, and the electric dipoles will be aligned along the direction of the electric field, and will reach an equilibrium state after spinning (Fig. 4a <i>). Then switch on the external circuit. When pressure is applied to the membrane, the spontaneous polarization strength of the membrane will decrease, and the charge induced on the electrode will also decrease accordingly. The excess charge flows through the circuit to form a current (Fig. 4a <ii>). When the pressure disappears, the spontaneous polarization strength of the membrane returns to its original state, and the flowing charge returns to the electrode to form a reverse current (Fig. 4a <iii>). In this configuration, the PDRC material will no longer be hindered by the electrode layer, thus achieving compatibility between PDRC and piezoelectric monitoring. It is worth noting that the single electrode output performance of PVDF-HFP is very dependent on the integrity of the PVDF-HFP layer. If the PVDF-HFP fiber membrane is damaged, which causes the drop of its PDRC performance, there will be a significant drop of the electric output, which can be used to monitoring the function of PDRC.

This nanogenerator has high sensitivity and can detect a minimum force of 0.1 N. Moreover, the output increases as the pressure increases, as shown in Fig. 4b, c. Therefore, all human activities and even small animal activities on the roof can be monitored. In order to easily estimate the piezoelectric power of the nanogenerator, the output under different external load resistances was measured. As shown in Fig. 4d. The pressure was maintained at 170 N. As the external load increases, the current gradually decreases and the voltage gradually increases. And then, the power of nanogenerator can be calculated by using these data. As shown in Fig. 4e, the dependence of output power on load resistances, when the load resistance is 100 MΩ, the output power reaches the maximum value of 0.3 W m^{-2}. Its output performance is significantly higher than other piezoelectric nanogenerators, which has obvious advantages. The comparison results are shown in Table S2.

Then, PDRC's self-monitoring function was confirmed. A 2 × 2 PDRC array was fabricated, the area 2 was artificially damaged (Fig. 4f), and the heat dissipation function was seriously affected. However, it can be easily seen from the electrical signals of the PDRC array in Fig. 4g that the working status of each area. And it can be accurately determined that areas 2 is damaged and needs repair. The sensitivity of the damage monitor is shown in Fig. S2. On the other hand, the pyroelectric properties [35] of PVDF-HFP when irradiated by sunlight are also very helpful to PDRC's self-monitoring function. As shown in Fig. 4h, when the radiant cooler is blocked by an object, the output electrical signal will have a significant change. When the obstruction is removed, a reverse signal will appear. So as to realize the self-monitoring of whether the radiant cooler is blocked.

3.3. Real-time monitoring of rainfall

The piezoelectric effect of PVDF-HFP broadens the function of the PDRC, enabling it to not only perform passive radiative cooling on hot days, but also collect the mechanical energy of raindrops on rainy days and monitor the rainfall level in real time. At the same time, the working state of each area can be accurately monitored through the monitoring system, and accurate and intuitive feedback can be obtained for the damage of a certain area, so that the PDRC can be intelligent. Its schematic is shown in Fig. 5a. There are many ways to judge the rainfall level, which can be based on the size of the raindrops or the rainfall. Because raindrops are affected by air resistance during the falling process, they will eventually fall at a uniform speed. Different sizes of raindrops have different ending speeds, and the pressure generated by the drops falling on the roof is also different. Therefore, the

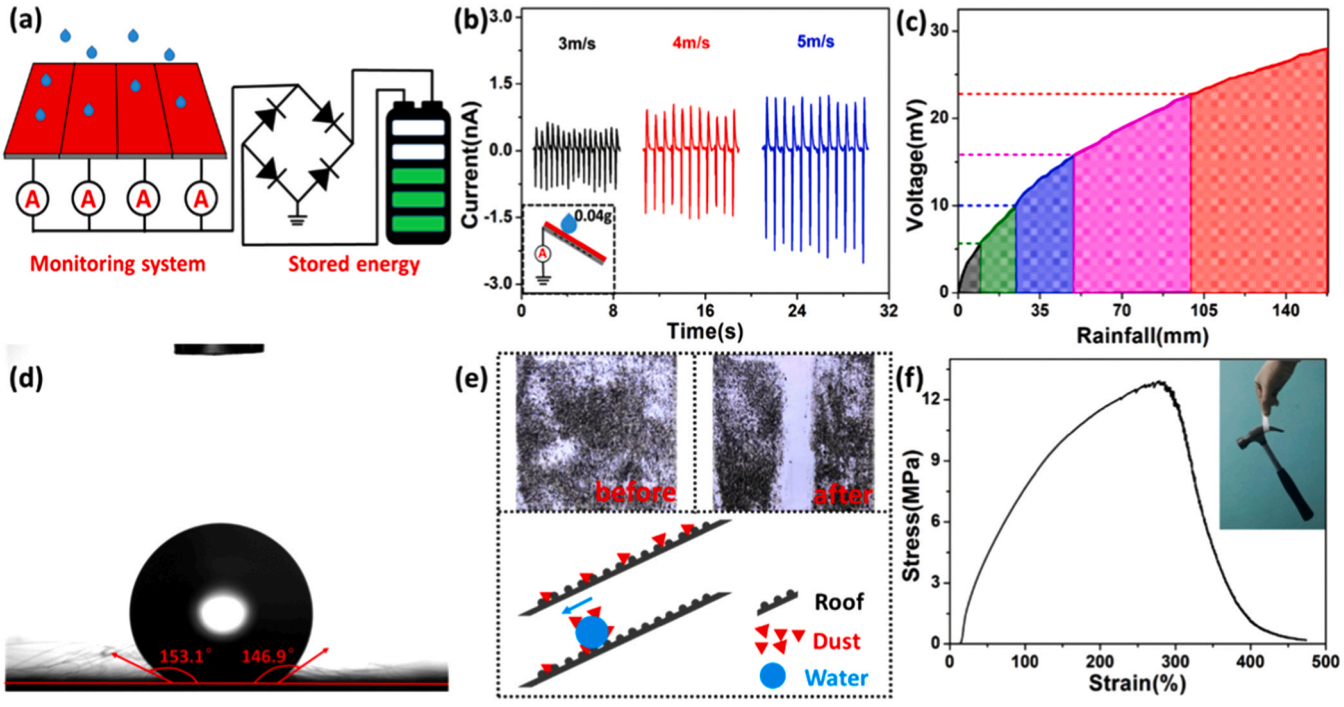

Fig. 5. Real-time monitoring of rainfall and its physical properties. (a) Schematic diagram of intelligent PDRC collecting raindrop mechanical energy and monitoring rainfall level in real time. (b) Output current when raindrops of different closing speeds fall on the roof. (c) Capacitor charging voltage corresponding to different rainfall. (d) The water contact angle of PVDF-HFP membrane. (e) The photograph and schematic of PVDF-HFP membrane self-cleaning ability. (f) Stress-strain curve for a 130 μm thick PVDF-HFP membrane. Inset shows a freestanding PVDF-HFP membrane of 10 mm width and 130 μm thickness supporting a hammer.

nanogenerator will have different output, according to the size of the output, rainfall level can be judged intuitively. As shown in Fig. 5b. The illustration is the schematic of the measurement. In order to easily obtain raindrops of different speeds, water droplets of the same size are dropped from different heights. Another way to judge the rainfall level is to calculate the rainfall. The more rainfall, the higher the rainfall level. Nanogenerator can convert the mechanical energy of raindrops into electrical energy and store them in capacitors through a rectifier circuit. The more rainfall, the more electrical energy is stored, and the higher the voltage of the capacitor (Fig. 5c). So it is easy to judge the rainfall and the rainfall level through the capacitor voltage.

On the other hand, the addition of hexafluoropropylene increases the flexibility of PVDF-HFP products, which is conducive to the combination with electrodes, and at the same time improves its hydrophobicity, which is more conducive to realization self-cleaning. It can be seen from Fig. 5d, the water contact angle of the PVDF-HFP membrane, that the membrane has a high hydrophobic angle. However, a higher hydrophobic angle is beneficial for the self-cleaning function of the roof. Fig. 5e shows the self-cleaning ability of the roof and the microscopic principle. When water flows from the surface of the membrane, the dust on the surface of the membrane will be absorbed by the water droplets and taken away to achieve the purpose of cleaning. As a roof layer, PVDF-HFP membrane also needs to have good mechanical strength. Fig. 5f shows the stress-strain curve of the membrane. It can be seen that the membrane can withstand a maximum stress of 12 MPa and has good mechanical properties.

Any outdoor coating has the problem of aging, falling off and becoming dirty, thus generating a lot of construction waste. The heat dissipation material in this work is entirely composed of polymer fibers, so the damaged coating can be re-dissolved and recycled by acetone-DMF solution. As shown in Fig. 6a, with the addition of acetone-DMF dissolution, the fiber membrane was gradually dissolved. Even after getting dirty, the supernatant can be used to reshape the fiber membrane (Fig. 6b). The recyclability of the thermal coating brings additional benefits to its green and energy-saving features.

4. Conclusions

In summary, we have successfully developed an effective intelligent PDRC dual energy-saving design based on electrospinning PVDF-HFP fiber. On the one hand, it is a simple, efficient and low-cost passive daytime radiative cooling technology that uses cold space as a sink for cooling. The PVDF-HFP micro-nano fibers prepared by electrospinning can reflect sunlight well (0.3–2.5 μm), and can radiate heat to the outside space through the atmospheric windows (8–13 μm and 16–20 μm), thus achieving the highest temperature drop of 10 °C. On the other hand, the PVDF-HFP fiber membranes have excellent piezoelectric properties in single electrode configuration, and the output power is up to 0.3 W m^{-2} under 170 N pressure. It can efficiently collect mechanical energy in the environment, even the mechanical energy of 0.04 g raindrops, and realize self-powered pressure sensing, self-monitoring of the PDRC and real-time monitoring of rainfall levels. Through the designed circuit, the working status of each area can be clearly monitored. The very important thing is that the superhydrophobic property of PVDF-HFP allows the intelligent roof to clean itself, which greatly reduces the difficulty of roof cleaning. The worn membrane can be re-dissolved to be re-electrospun into new membrane, which reduces residual polymer materials to avoid environment pollution. The use of hand-held electrospinning device is simple and easy in the preparation process, which can be used for fixing the broken area of the membrane. Therefore, in the future large-scale production and intelligent housing applications, the proposed technology has high competitiveness and huge development potential.

CRediT authorship contribution statement

Wei-Zhi Song: Investigation, Writing - original draft. **Xiao-Xiong Wang:** Conceptualization, Resources. **Hui-Jing Qiu:** Formal analysis. **Ning Wang:** Formal analysis. **Miao Yu:** Visualization. **Zhiyong Fan:** Visualization. **Seeram Ramakrishna:** Funding acquisition. **Han Hu** : Visualization. **Yun-Ze Long:** Supervision, Funding acquisition.

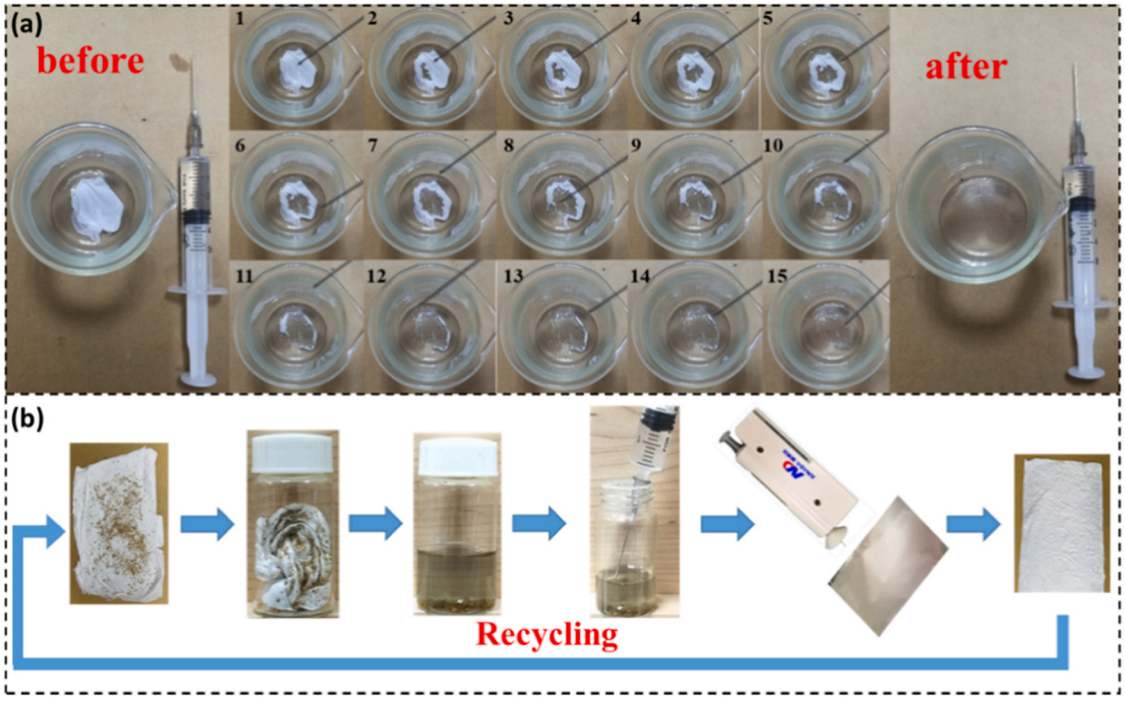

Fig. 6. Recycling of waste fiber membrane.

Declaration of Competing Interest

The authors declare that they have no known competing financial interests or personal relationships that could have appeared to influence the work reported in this paper.

Acknowledgments

This work was supported by the National Natural Science Foundation of China (51973100 and 51673103), State Key Laboratory of Bio-Fibers and Eco-Textiles, Qingdao University (RZ2000003334), and the National Key Research Development Project (2019YFC0121402).

Appendix A. Supporting information

Supplementary data associated with this article can be found in the online version at doi:10.1016/j.nanoen.2020.105695.

References

[1] J. Mandal, Y. Fu, A. Overvig, M. Jia, K. Sun, N. Shi, H. Zhou, X. Xiao, N. Yu, Y. Yang, Hierarchically porous polymer coatings for highly efficient passive daytime radiative cooling, Science 362 (2018) 315–319.
[2] Z.F. Huang, X.L. Ruan, Nanoparticle embedded double-layer coating for daytime radiative cooling, Int. J. Heat Mass Transf. 104 (2017) 890–896.
[3] B. Bhatia, A. Leroy, Y.C. Shen, L. Zhao, M. Gianello, D.H. Li, T. Gu, J.J. Hu, M. Soljacic, E.N. Wang, Passive directional sub-ambient daytime radiative cooling, Nat. Commun. 9 (2018) 5001.
[4] N. Li, J.F. Wang, D.F. Liu, X. Huang, Z.K. Xu, C.Y. Zhang, Z.J. Zhang, M.F. Zhong, Selective spectral optical properties and structure of aluminum phosphate for daytime passive radiative cooling application, Sol. Energy Mater. Sol. Cells 194 (2019) 103–110.
[5] T.S. Eriksson, S.-J. Jiang, C.G. Granqvist, Surface coatings for radiative cooling applications: Silicon dioxide and silicon nitride made by reactive rf-sputtering, Sol. Energy Mater. 12 (1985) 319–325.
[6] M.M. Hossain, B. Jia, M. Gu, A metamaterial emitter for highly efficient radiative cooling, Adv. Opt. Mater. 3 (2015) 1047–1051.
[7] Q. Liu, W.C. Wu, S.H. Lin, H. Xu, Y.H. Lu, W.J. Song, Non-tapered metamaterial emitters for radiative cooling to low temperature limit, Opt. Commun. 450 (2019) 246–251.
[8] S. Fan, Thermal photonics and energy applications, Joule 1 (2017) 264–273.
[9] L. Zhu, A.P. Raman, S. Fan, Radiative cooling of solar absorbers using a visibly transparent photonic crystal thermal blackbody, Proc. Natl. Acad. Sci. 112 (2015) 12282–12287.
[10] A.R. Gentle, G.B. Smith, Radiative heat pumping from the earth using surface phonon resonant nanoparticles, Nano Lett. 10 (2010) 373–379.
[11] C.G. Granqvist, A. Hjortsberg, Surfaces for radiative cooling: silicon monoxide films on aluminum, Appl. Phys. Lett. 36 (1980) 139–141.
[12] Z. Chen, L. Zhu, A. Raman, S. Fan, Radiative cooling to deep sub-freezing temperatures through a 24 h day–night cycle, Nat. Commun. 7 (2016) 13729.
[13] W. Li, Y. Shi, K.F. Chen, L.X. Zhu, S.H. Fan, A comprehensive photonic approach for solar cell cooling, ACS Photonics 4 (2017) 774–782.
[14] A.P. Raman, M.A. Anoma, L. Zhu, E. Rephaeli, S. Fan, Passive radiative cooling below ambient air temperature under direct sunlight, Nature 515 (2014) 540–544.
[15] Y. Zhai, Y. Ma, S.N. David, D. Zhao, R. Lou, G. Tan, R. Yang, X. Yin, Scalable-manufactured randomized glass-polymer hybrid metamaterial for daytime radiative cooling, Science 355 (2017) 1062–1066.
[16] A.R. Gentle, G.B. Smith, A subambient open roof surface under the mid-summer sun, Adv. Sci. 2 (2015), 1500119.
[17] X. Wang, X.H. Liu, Z.Y. Li, H.W. Zhang, Z.W. Yang, H. Zhou, T.X. Fan, Scalable flexible hybrid membranes with photonic structures for daytime radiative cooling, Adv. Funct. Mater. 30 (2020), 1907562.
[18] X.X. Wang, W.Z. Song, M.H. You, J. Zhang, M. Yu, Z.Y. Fan, S. Ramakrishna, Y. Z. Long, Bionic single-electrode electronic skin unit based on piezoelectric nanogenerator, ACS Nano 12 (2018) 8588–8596.
[19] J.H. Zhang, Y. Li, J.H. Du, X.H. Hao, Q. Wang, Bio-inspired hydrophobic/cancellous/hydrophilic Trimurti PVDF mat-based wearable triboelectric nanogenerator designed by self-assembly of electro-pore-creating, Nano Energy 61 (2019) 486–495.
[20] C.K. Jeong, D.Y. Hyeon, G.T. Hwang, G.J. Lee, M.K. Lee, J.J. Park, K.I. Park, Nanowire-percolated piezoelectric copolymer-based highly transparent and flexible self-powered sensors, J. Mater. Chem. A 7 (2019) 25481–25489.
[21] A. Greiner, J.H. Wendorff, Electrospinning: a fascinating method for the preparation of ultrathin fibers, Angew. Chem. Int. Ed. 46 (2007) 5670–5703.
[22] N. Bhardwaj, S.C. Kundu, Electrospinning: a fascinating fiber fabrication technique, Biotechnol. Adv. 28 (2010) 325–347.
[23] B. Sun, Y.Z. Long, Z.J. Chen, S.L. Liu, H.-D. Zhang, J.C. Zhang, W.P. Han, Recent advances in flexible and stretchable electronic devices via electrospinning, J. Mater. Chem. C 2 (2014) 1209–1219.
[24] H.J. Qiu, W.Z. Song, X.X. Wang, J. Zhang, Z. Fan, M. Yu, S. Ramakrishna, Y. Z. Long, A calibration-free self-powered sensor for vital sign monitoring and finger tap communication based on wearable triboelectric nanogenerator, Nano Energy 58 (2019) 536–542.
[25] X. Wang, H. Xiang, C. Song, D. Zhu, J. Sui, Q. Liu, Y.Z. Long, Highly efficient transparent air filter prepared by collecting-electrode-free bipolar electrospinning apparatus, J. Hazard. Mater. 385 (2020), 121535.
[26] S. Thenmozhi, N. Dharmaraj, K. Kadirvelu, H.Y. Kim, Electrospun nanofibers: New generation materials for advanced applications, Mater. Sci. Eng. B 217 (2017) 36–48.
[27] J. Yoon, H.S. Yang, B.S. Lee, W.R. Yu, Recent progress in coaxial electrospinning: new parameters, various structures, and wide applications, Adv. Mater. 30 (2018), 1704765.
[28] Y. Liao, C.H. Loh, M. Tian, R. Wang, A.G. Fane, Progress in electrospun polymeric nanofibrous membranes for water treatment: fabrication, modification and applications, Prog. Polym. Sci. 77 (2018) 69–94.
[29] J.S. Tan, Y.Z. Long, M.M. Li, Preparation of aligned polymer micro/nanofibres by electrospinning, Chin. Phys. Lett. 25 (2008) 3067–3070.
[30] C. Chang, V.H. Tran, J. Wang, Y.-K. Fuh, L. Lin, Direct-write piezoelectric polymeric nanogenerator with high energy conversion efficiency, Nano Lett. 10 (2010) 726–731.
[31] J. Chang, M. Dommer, C. Chang, L. Lin, Piezoelectric nanofibers for energy scavenging applications, Nano Energy 1 (2012) 356–371.
[32] M.H. You, X.X. Wang, X. Yan, J. Zhang, W.Z. Song, M. Yu, Z.Y. Fan, S. Ramakrishna, Y.Z. Long, A self-powered flexible hybrid piezoelectric–pyroelectric nanogenerator based on non-woven nanofiber membranes, J. Mater. Chem. A 6 (2018) 3500–3509.
[33] S.C. Xu, C.C. Qin, M. Yu, R.H. Dong, X. Yan, H. Zhao, W.P. Han, H.D. Zhang, Y. Z. Long, A battery-operated portable handheld electrospinning apparatus, Nanoscale 7 (2015) 12351–12355.
[34] J. Fang, H. Niu, H. Wang, X. Wang, T. Lin, Enhanced mechanical energy harvesting using needleless electrospun poly(vinylidene fluoride) nanofibre webs, Energy Environ. Sci. 6 (2013) 2196–2202.
[35] A. Thakre, A. Kumar, H.C. Song, D.Y. Jeong, J. Ryu, Pyroelectric energy conversion and its applications—flexible energy harvesters and sensors, Sensors 19 (2019) 2170.